Pattern Formation in Nanoparticle Assemblies via Directed Solvent Dewetting- Auxiliary Material

Christopher P. Martin[*1], Matthew O. Blunt[*1], Emmanuelle Pauliac-Vaujour[1], Andrew Stannard[1], Ioan Vancea[2], Uwe Thiele[2], and Philip Moriarty[1]

[1]School of Physics and Astronomy, The University of Nottingham, University Park, Nottingham NG7 2RD, UK. [2]Max Planck Institute for the Physics of Complex Systems, Nöthnitzer Str. 38, D-01187 Dresden, Germany. [*]These authors contributed equally to this work.

The structure in Fig. S1a (which is an extended version of the image in the main paper (Fig. 1(a))) appears to exhibit two different length scales of cellular network. Although this may seem visually obvious, the brain has a tendency to seek out order and to look for patterns. Sometimes therefore patterns can be misinterpreted, and an analytical confirmation is worthwhile in this case. Fig. S1b shows a radially-averaged two-dimensional fast Fourier transform (2DFFT) of the image in Fig. S1a. Although the data are a little noisy, two peaks are clearly visible. A fit by locally-weighted scatter-plot smoothing (LOWESS) clarifies the shape of the curve, and highlights the two peaks, which indicate two distinct length scales.

Although the 2DFFT is well-suited to analysing the length-scales within an image, to obtain a reliable comparison of two images requires a more detailed statistical analysis. Fig. S2a shows a Voronoi tessellation[1] superimposed onto the AFM image from Fig. 1. This is simply a reduction of the cellular network into a series of polygons. There are two significant quantities associated with such a tessellation: the *variance* (μ_2) and the *entropy* (S) of the distribution of the number of cell sides. The details of these measures are described elsewhere[1], but the important fact is that they define the degree of disorder of a cellular structure. A Voronoi tessellation created from a completely

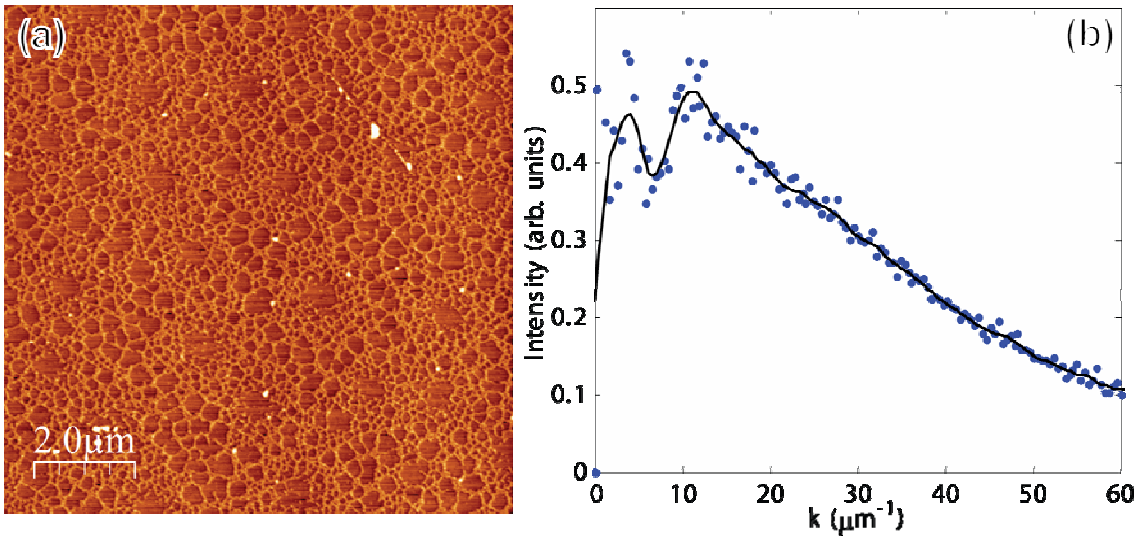

Figure S1 (a) An atomic force microscope (AFM) image of a two-level cellular structure formed by spin-casting a solution of gold nanoparticles in toluene onto a silicon substrate, and (b) a radially-averaged two-dimensional fast Fourier transform of (a), with the original "binned" data shown as filled circles. The solid line is the same data after smoothing by a 10-point "LOWESS" method, which clarifies the bimodal nature of the distribution.

random distribution of points will have μ_2=1.78 and S=1.71, whereas common values for single length-scale nanoparticle cellular networks are μ_2~1.0 and S~1.4. Both the experimental and simulated networks in Fig. S2 have μ_2=1.3 and S=1.5 within error (the magnitude of the error was obtained by manually re-defining the cell centres several times and observing the resulting maximum variation in the parameters).

Although the Voronoi tessellation gives a good numerical comparison of cellular structures (and indeed point distributions), a technique that is yet more detailed and robust is Minkowski functional grain-growth analysis[2-3]. Fig. S3 shows the result of this analysis, including a comparison with a single length-scale network and a random network. It is clear from these plots that the two structures are statistically equivalent.

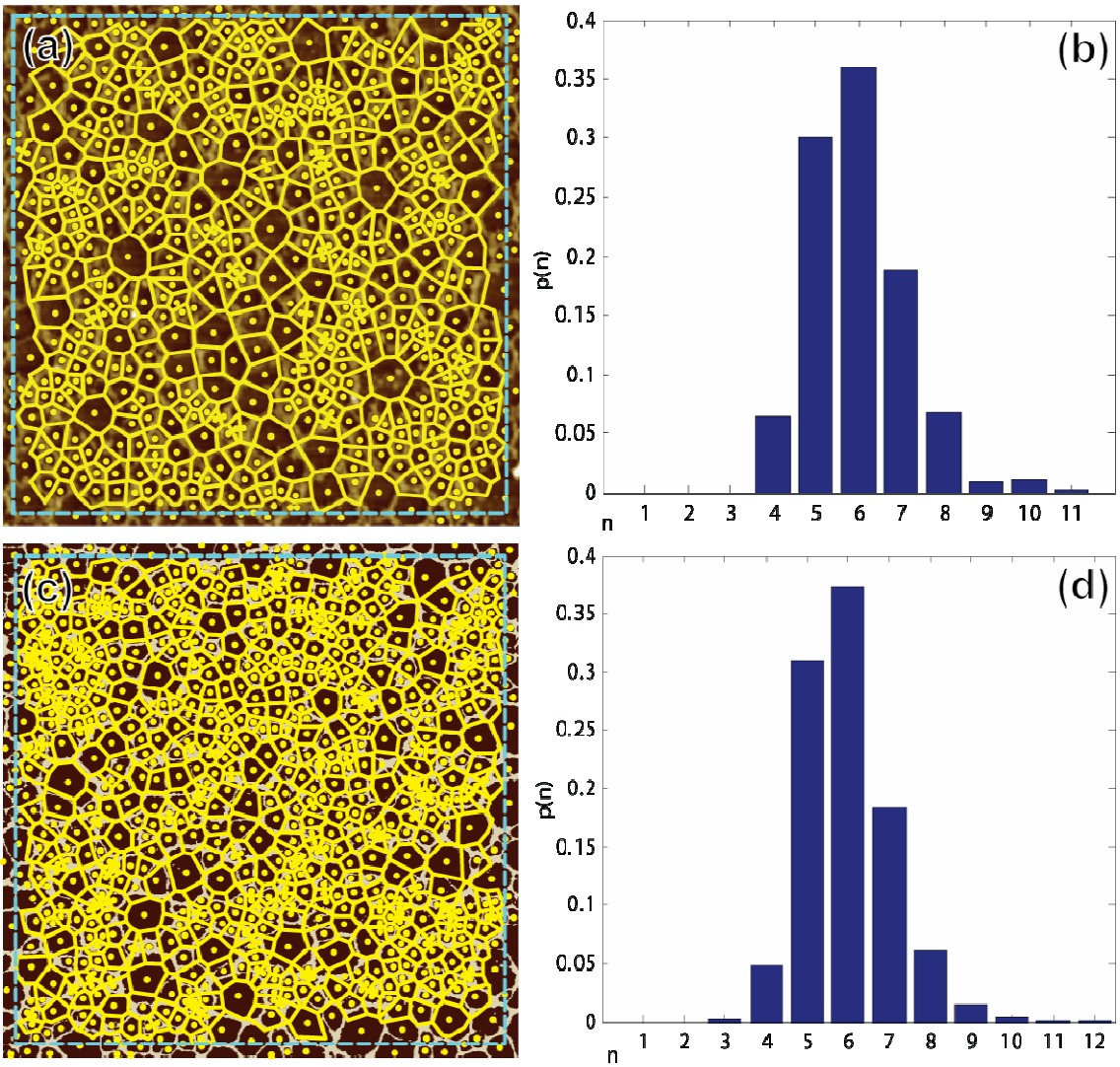

Figure S2 (a) The AFM image from Fig. 1(a) with a Voronoi tessellation[1] superimposed, (b) a plot of the frequency distributions of cells with a given number of sides for the tessellation in (a), having a variance of 1.3±0.1, and an entropy of 1.50±0.06, (c) a simulation image with a coupling between μ and solvent coverage with a superimposed Voronoi tessellation, and (d) a plot of the frequency distributions of cells with a given number of sides for the tessellation in (c), having a variance of 1.3±0.1, and an entropy of 1.48±0.06.

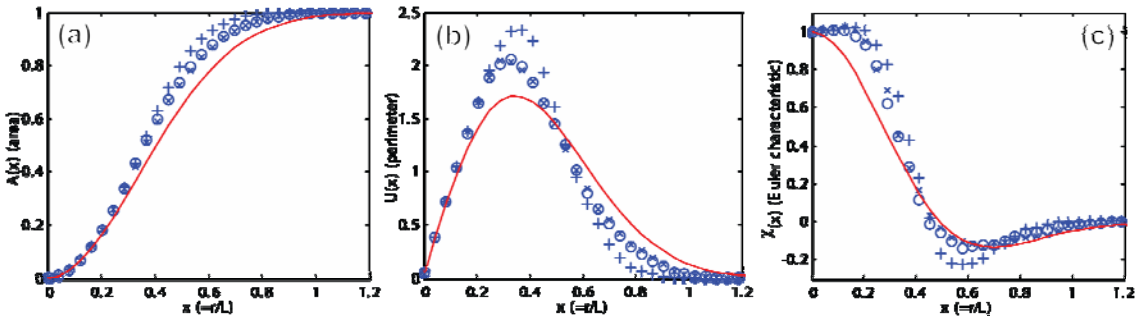

Figure S3 Square-grain Minkowski functional comparison[2-3] of the structures in Fig. S2 (a) and (b), showing the experimental data as crosses, simulated data as open circles, and for the purposes of comparison, data from a single-length-scale network is shown as plus symbols, and the solid line represents the theoretical result for a purely random distribution.

Nucleating Dewetting

Fig. S4 on the following page supplements Figs. 2 and 3 in the paper, showing that nanoparticle rings (similar to those discussed by Ohara and Gelbart[4] and Maillard et al.[5] (and recently simulated by Yosef and Rabani[6])) are induced along the edges of an AFM-generated oxide square on H:Si(111). The solvent for the nanoparticles in this case was dichloromethane. Although the image quality is not particularly high, note the absence of nanoparticle rings in areas other than along the edges of the oxide. Moreover, the majority of the rings are centred on the lines of oxide forming the edges of the square. As discussed in the paper, the oxide lines lead to rupture of the nanoparticle-solvent film. The nucleated hole grows and nanoparticles are carried with the dewetting solvent front, leaving a ring of nanoparticles when the solvent completely evaporates.

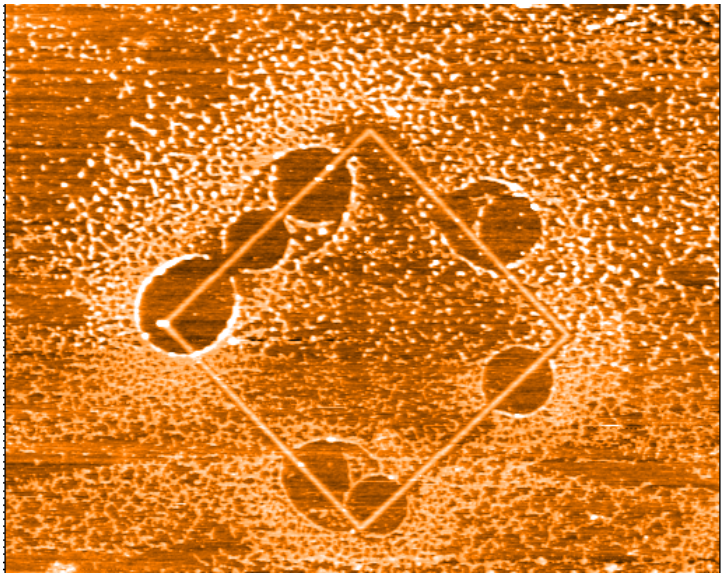

Fig. S4. An 8μm x 10 μm AFM image showing the formation of nanoparticle rings due to solvent dewetting driven by lines of oxide on H:Si(111). The retreating solvent front carries nanoparticles with it and ultimately leads to the production of the nanoparticle rings observed in the image.

References

1. Weaire, D. and Rivier, N. Soap, cells and statistics - random patterns in two dimensions. *Contemp. Phys.* **25**, 59-99 (1984).

2. Michielsen, K. and De Raedt, H. Integral-Geometry Morphological Image Analysis. *Physics Reports* **347**, 461-538 (2001).

3. Frehill, F. et al. Iron Wheels on Silicon: Wetting Behavior and Electronic Structure of Adsorbed Organostannoxane Clusters. *Langmuir* **20**, 6421-6429 (2004).

4. P. C. Ohara and W. M. Gelbart, *Langmuir* **14** 3418 (1998)

5. M. Maillard, L. Motte, and M. P. Pileni, *Adv. Mater.* **13** 200 (2001)

6. G. Yosef and E. Rabani, *J. Phys. Chem. B* **110** 20965 (2006)